APPLICATION OF CONTINUOUS WAVELET TRANSFORMS TO THE ANALYSIS OF EXPERIMENTAL TURBULENT VELOCITY SIGNALS

Guido Buresti
Department of Aerospace Engineering, University of Pisa
Via Diotisalvi 2, 56126 Pisa, Italy

Giovanni Lombardi
Department of Aerospace Engineering, University of Pisa
Via Diotisalvi 2, 56126 Pisa, Italy

ABSTRACT

Processing procedures based on the continuous complex wavelet transform are applied to the analysis of velocity signals obtained in a developing turbulent flow. It is shown that the frequencies contributing to the energy and to the Reynolds stresses may be characterized better than with Fourier analysis. Indeed, the time variation of the contribution of the different frequencies to the energy of the fluctuations and to the Reynolds stresses may be singled out, so that it may be ascertained if these contributions are simultaneous or alternative, continuous or intermittent. In particular, it is shown that in certain positions at the end of the potential cores of a coaxial jet high energy fluctuations, probably connected to the passage of rolled-up vortical structures, may produce low values of the Reynolds stress because their contribution to correlation oscillates in time between positive and negative values. Examples of the application of different types of wavelet dynamical filters are also given, and a wavelet local correlation coefficient is defined.

INTRODUCTION

The wavelet transform allows a signal to be described by means of oscillating, zero-mean, base functions of compact support, i.e. whose values are zero or negligible outside a certain time interval, which defines the "scale" of the wavelet. By a process of convolution of the signal with dilated versions of these basic wavelets, the wavelet transform coefficients provide an evaluation of the "instantaneous" similarity of the signal with wavelets of different scale. By appropriately connecting scales and inverse frequencies, it is thus possible to obtain the time variation of the contribution of the different frequencies to various physical quantities connected with the signal (e.g. its energy or its correlation with another signal). This analysis is particularly suited when the fluctuations of a signal derive, rather than from the sum of infinite sinusoidal waves, from the sum of finite "events", i.e. when the signal is intrinsically intermittent, as is indeed the case for most turbulent velocity fields.

The theory of wavelet transforms, both continuous and discrete, has been thoroughly developed in recent years (see Daubechies, 1992), and applied in different fields of physics and engineering. Several applications of the wavelet transform to the analysis of turbulent velocity signals are present in the literature (see, e.g., Farge et al., 1996). In most of these applications, wavelet-based procedures are used to enhance the flow field structures containing most of the turbulent energy, to evaluate their scales and to characterize the degree of intermittence of their occurrence.

Cross-correlation techniques based on the continuous complex-wavelet transform have also been introduced (Onorato et al., 1997), and tested by processing velocity signals obtained from axisymmetric direct numerical simulations of a coaxial jet flow at low Reynolds numbers. By applying these procedures to the signals representing two velocity components simultaneously obtained at the same point of the flow, it was possible to derive the time variation of the contribution of the single scales to the relevant Reynolds stress. Thus it could be ascertained whether a certain value of the Reynolds stress at a point of the flow was produced by an almost time-constant contribution, or by an intermittent one.

The main object of the present paper is to study the performance of these and other wavelet-based techniques for the analysis of experimental turbulent velocity signals obtained at higher Reynolds numbers than those attainable through DNS.

GENERALITIES ON WAVELET TRANSFORMS

A wavelet can be any real or complex valued function $\psi(t) \in L^2$ of compact support that satisfies the following *admissibility condition*:

$$C_\psi = \int_{-\infty}^{\infty} |\hat{\psi}(\omega)|^2 |\omega|^{-1} d\omega < \infty \qquad (1)$$

where C_ψ is the *admissibility constant*, and $\hat{\psi}(\omega)$ is the Fourier transform of $\psi(t)$. This condition implies, in practice, that $\psi(t)$ has zero mean value.

The continuous wavelet transform of a function $f(t)$ is defined as the convolution between f and dilated versions of the wavelet:

$$W_f(a,\tau) = \frac{1}{\sqrt{a}} \int_{-\infty}^{\infty} f(t) \psi^*\left(\frac{t-\tau}{a}\right) dt \qquad (2)$$

where $a \in \Re^+$ is the scale dilation parameter, $\tau \in \Re$ is the translation parameter corresponding to the position of the wavelet in the physical space, and the symbol * indicates the complex conjugate.

The wavelet functions are not orthogonal and the continuous transform is highly redundant, but, thanks to the admissibility condition, an inversion formula exists to recover $f(t)$ from its wavelet coefficients (Daubechies, 1992). In the present study the complex Morlet wavelet ($\psi(t) = e^{i\omega_0 t} e^{-t^2/2}$) is used. Although this wavelet does not exactly satisfies (1), if we take $\omega_o = 6$ it becomes admissible and progressive (i.e. with $\hat{\psi}(\omega) = 0$ for $\omega < 0$) within typical computer round-off accuracy. It is possible to relate scales and frequencies, and for the Morlet wavelet this relation is $f = \omega_o/(2\pi a)$.

From the wavelet transform one obtains time-scale maps (*scalograms*), giving e.g. the modulus and phase of the transform (if the wavelet is complex).

Let $W_f(a,\tau)$ and $W_g(a,\tau)$ be, respectively, the wavelet transforms of $f(t)$ and $g(t)$. We define the *wavelet cross-scalogram* as follows:

$$W_{fg}(a,\tau) = W_f^*(a,\tau) W_g(a,\tau) \qquad (3)$$

When the analysing wavelet is complex, $W_{fg}(a,\tau)$ is also complex; if $CoW_{fg}(a,\tau)$ is its real part (*co-scalogram*), it can be shown that (Onorato et al., 1997)

$$\int_{-\infty}^{\infty} f(t) g(t)\, dt = \left(1/C_\psi\right) \int_0^{\infty} \int_{-\infty}^{\infty} CoW_{fg}(a,\tau)\, d\tau\, da/a^2 \qquad (4)$$

If $f = g$, relations (3) and (4) show that the square modulus of the wavelet transform gives the contribution of each scale to the energy of the signal as a function of time. On the other hand, if $f(t)$ and $g(t)$ are two components of the velocity fluctuation at a certain point of a turbulent field, the co-scalogram can be used to detect time intervals and scales at which the contribution to the relevant Reynolds stress is significant. Also, for each scale (frequency) the angle of phase between the two signals may be found as a function of time (Onorato et al., 1997).

By integrating in time the functions $|W_f(a,\tau)|^2/C_\psi$ and $CoW_{fg}(a,\tau)/C_\psi$ we obtain, respectively, the *wavelet power spectrum* and the *wavelet co-spectrum*, which are smoother versions of their Fourier counterparts, being averages weighted by the power spectrum of the wavelet filter (Onorato et al., 1997, Perrier et al., 1995).

Once the different wavelet scalograms are available, their cross-sections at constant scale may be treated as time varying signals, and processed in order to extract more information on the behaviour of the flow. For instance, their statistical moments may be evaluated, as well as their correlation with different cross-sections of the same or of other scalograms (Li, 1998). Furthermore, by using thresholding procedures on a scalogram, masks may be produced and applied to the same or different scalograms. Thus different filters and conditional statistics may be obtained, having different physical meaning according to the used scalograms.

EXPERIMENTS AND ANALYSES

Processing techniques based on the complex Morlet wavelet are used in the present paper to analyse velocity signals obtained in a coaxial jet flow in a previous experimental investigation, described in more detail by Buresti et al. (1998). The analysed configuration has inner to outer jet diameter ratio $D_i/D_o \cong 0.5$ (D_o = 155 mm), a velocity ratio $U_i/U_o = 0.30$, and a sharp inner duct wall outlet. The outer jet velocity is U_o = 4 m/s, giving a Reynolds number $Re = U_o D_o/\nu = 4.2 \times 10^4$. In this flow condition, the potential cores of the two jets have comparable length, of the order of 3 D_i.

The axial and radial velocity components, u and v, were measured by means of X hot-wires placed inside the inner and outer shear layers, at several axial positions downstream of the jet outlet. Flow visualizations were also obtained using a pulsed Nd-YAG laser, by seeding the outer jet, and used as a guide in the interpretation of the analyses of the velocity signals, particularly as regards the role of the dynamics of the different vortical structures present in the near-field. Several methods of analysis based on the wavelet transform were used, viz.:

- Wavelet spectra and co-spectra, to determine the frequencies most contributing to the energy of the fluctuations and to the Reynolds stress production.
- Filtering of the energy maps through a filter mask based on suitable thresholding of the co-scalogram, to single out the portions of the velocity fluctuations most contributing to the Reynolds stresses.
- Introduction and analysis of the maps of a *Wavelet Local Correlation Coefficient*, defined as the ratio between the real part and the modulus of the relevant cross-scalogram:

$$WLCC(a,\tau) = \frac{CoW_{uv}(a,\tau)}{|W_{uv}(a,\tau)|} = \frac{CoW_{uv}(a,\tau)}{|W_u(a,\tau)||W_v(a,\tau)|} \qquad (5)$$

WLCC(a, τ) gives the local contribution of each frequency of the *u* and *v* fluctuations to their correlation coefficient.
- Application of a filter mask based on the modulus of the cross-scalogram $|W_{uv}(a, \tau)|$ to the maps of *WLCC(a, τ)*, and evaluation of the conditional statistics of their sections.

RESULTS

Figure 1 shows examples of the flow visualizations, viz. three instantaneous shots and the image obtained as an average of the whole set of acquired images. Different vortical structures are seen to be present at different times in the inner and outer shear layers, which may or not be synchronized and which are often characterized by a significant three-dimensionality. For sake of brevity, only the analyses of the velocity signals obtained at the two points shown in Fig. 1 d) will be described. Both points are well within the inner shear layer, and the second one is at the end of the potential cores of the two jets, a highly turbulent region where little information on the vortical structures can be derived from the visualizations.

Figure 2 shows, for point 1, the scalograms of the energy of the *u* and *v* fluctuations and their co-scalogram, limited to the frequency range containing appreciable values. Energy is seen to be prevailingly present around two frequencies, viz. 29 Hz and 81 Hz, even if with differences in relative importance in the two velocity components. Contributions to the *v* component energy are also present around 112 Hz, almost alternatively to those around 81 Hz, but, as can be seen from the co-scalogram, they give a limited contribution to the *u-v* correlation. Actually, a closer look at the maps shows that even the dominating frequencies, if derived from the local maxima of the maps, vary in time within small bands. This is physically explainable, considering that the distance between the vortices belonging to the same "family" is not exactly constant in time. Therefore, here and below, reference will be made to average dominating frequencies, generally coinciding with the maxima in the spectra or cross-spectra.

The integration in time of the maps of Fig. 2 produces the spectra and the co-spectrum of Fig. 3, which show the clear difference in relative energy content at the two dominating frequencies for the two velocity components, and the prevailing contribution of the higher one to their correlation. Also shown in this figure are the filtered energy spectra obtained by applying to the energy maps a mask derived by thresholding the absolute values of the co-scalogram with a threshold equal to 150% of the map

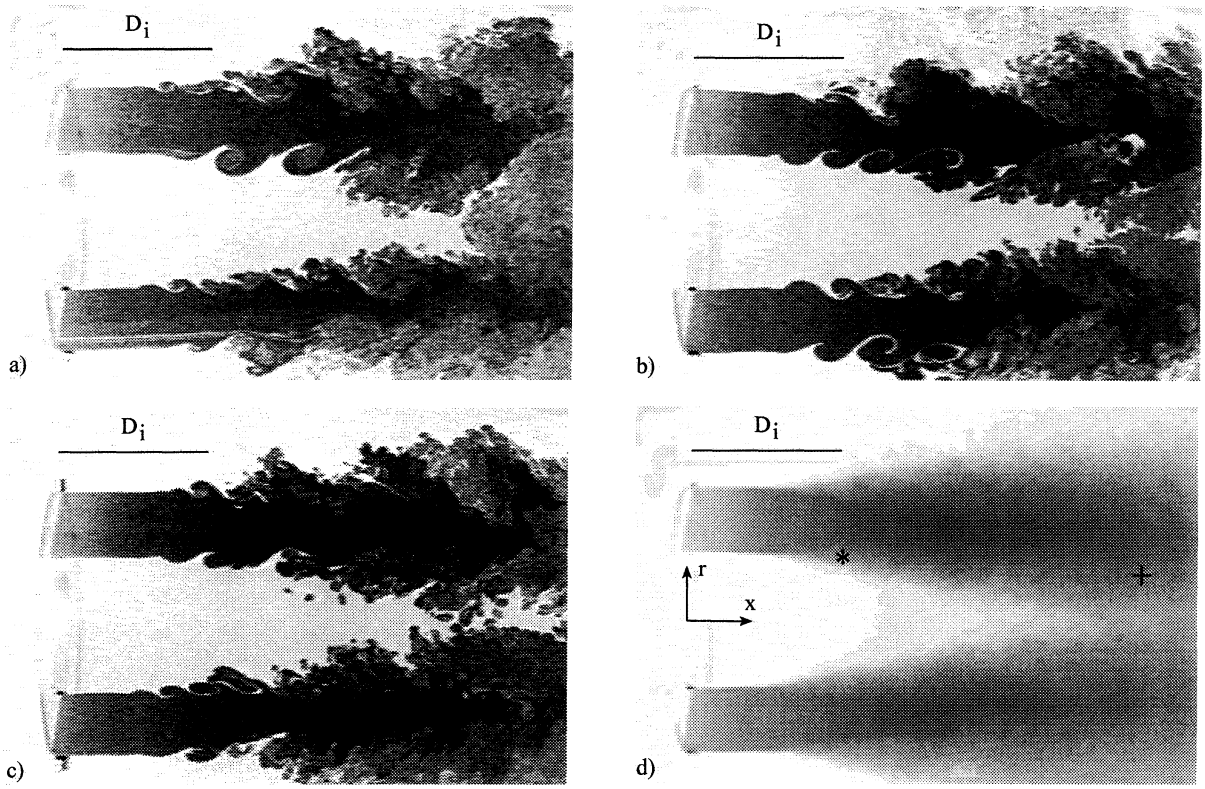

Figure 1. Examples of flow visualizations.
* Point 1: x/Di = 1.0, r/Di = 0.5; + Point 2: x/Di = 3.0, r/Di = 0.4.

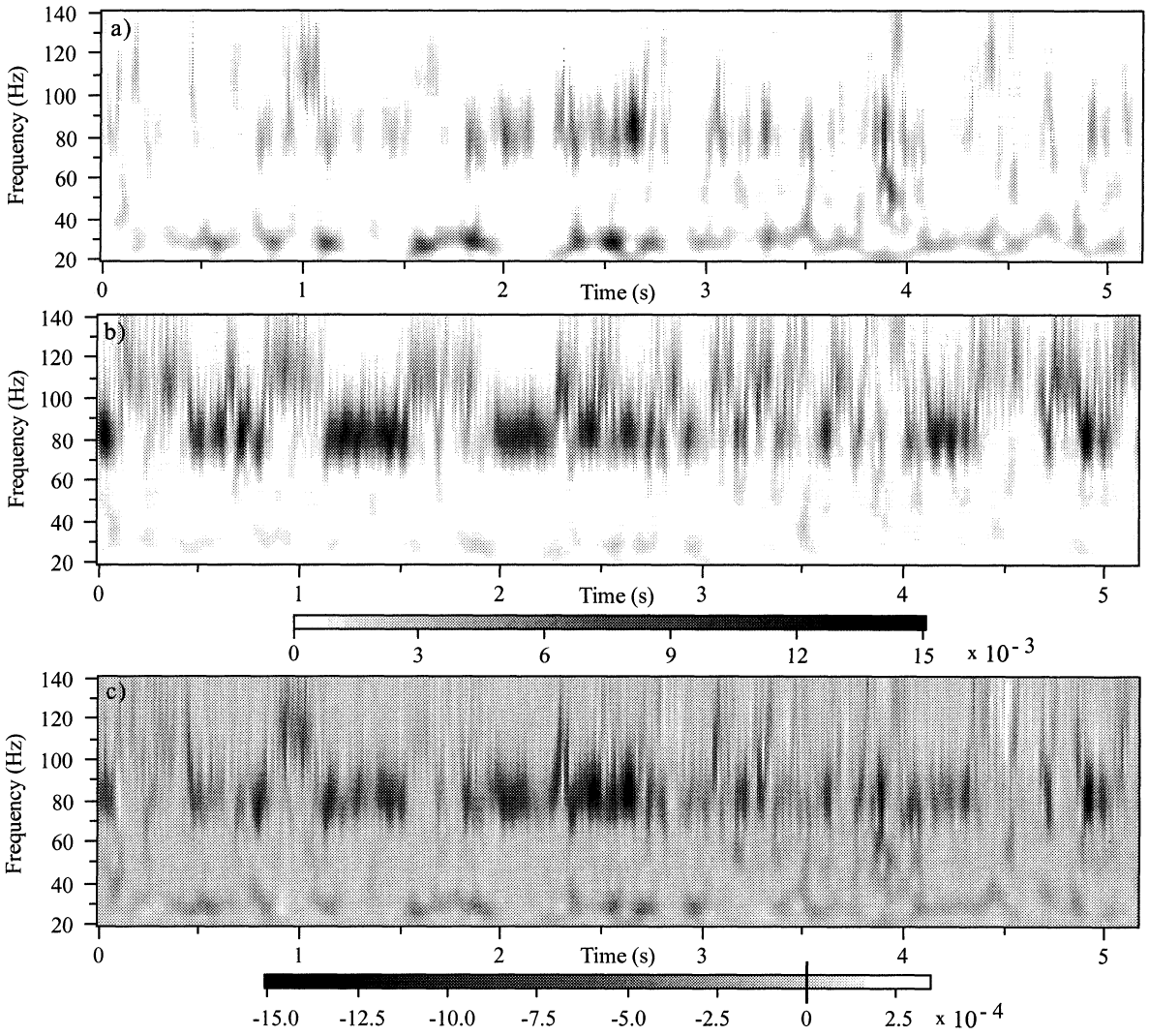

Figure 2. Scalograms of the energy of u (a) and v (b), and u-v co-scalogram (c). Point 1.

global average. Therefore, the filtered spectra indicate the portion of energy contributing most to the Reynolds stress; as can be seen, the filter acts prevailingly on the lower frequency for the u component, and on the frequencies above the higher peak for the v component.

As ascertained from the visualizations, and also from the analysis of the more downstream points, the two peaks in the spectra of Fig. 3 are linked to different "trains" of vortices that alternatively occur in the inner shear layer. The higher frequency peak corresponds to vortices deriving from a primary instability of the shear layer, as was verified by considering the Strouhal numbers based on the estimated thickness of the boundary layers at the jet exit. Conversely, the lower frequency scales on the jet core length, becomes more and more dominating moving downstream, and then undergoes the expected process of subharmonic enhancement connected with the mechanism of vortex pairing.

This interpretation agrees with the results obtained at $x/D_i = 2.0$ (not shown here), and with those of point 2, for which we show in Figure 4 the wavelet cross-spectrum and co-spectrum. In this position no significant energy is present around 81 Hz, the peak around 29 Hz has broadened significantly (in connection with a more intermittent and variable appearance), and a new peak around 15 Hz has appeared. It is most remarkable that only the latter peak dominates the co-spectrum, and thus contributes to the correlation. Obviously, the action of the filter based on the u-v co-scalogram is now prevailing on the higher frequency; however, the filtering action seems to be less than might have been expected from the negligible values of the co-spectrum at this frequency.

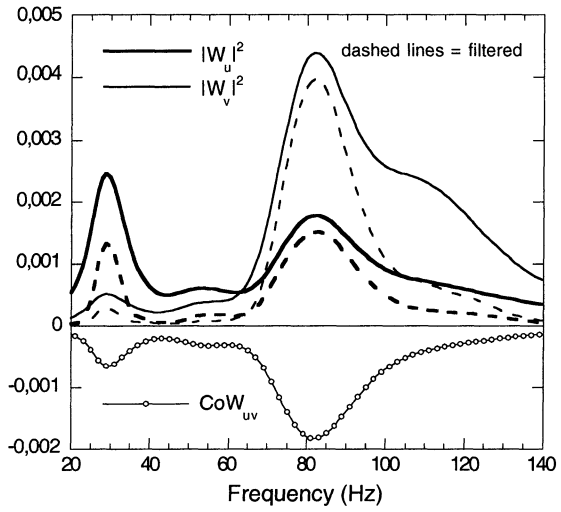

Figure 3. Wavelet energy spectra of *u* and *v*, and *u-v* co-spectrum for point 1.

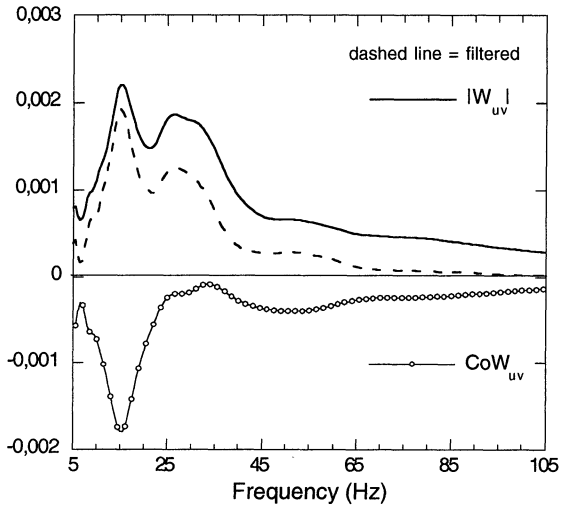

Figure 4. Wavelet *u-v* cross-spectrum and *u-v* co-spectrum for point 2.

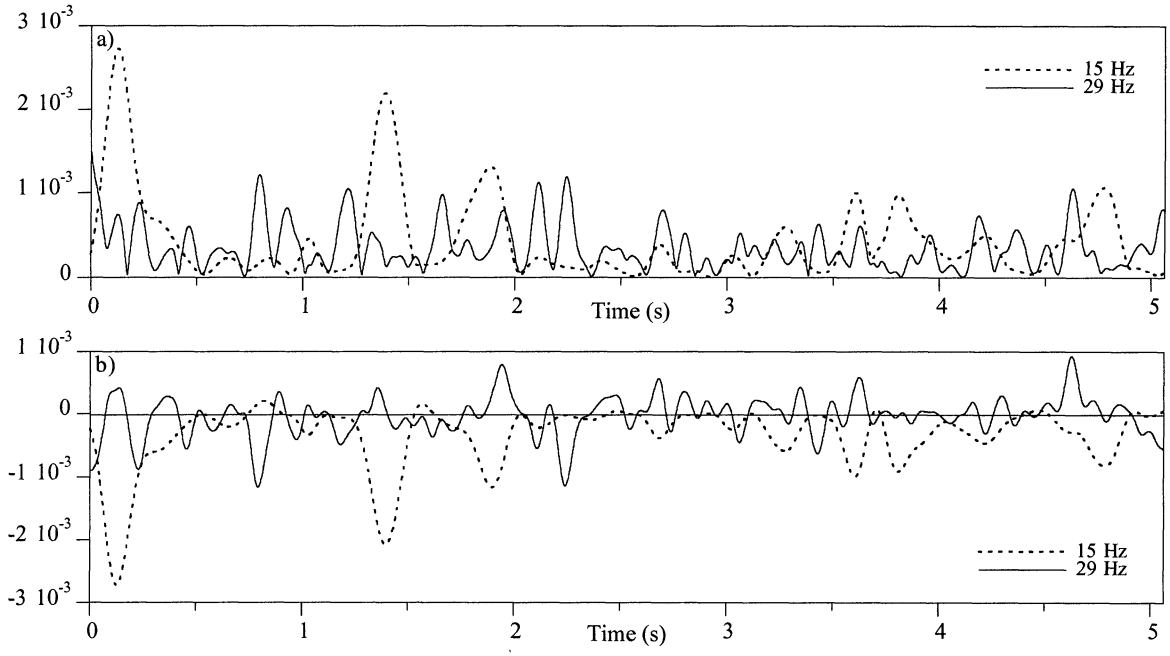

Figure 5. Sections of the *u-v* cross-scalogram (a) and *u-v* co-scalogram (b) at the dominating frequencies. Point 2.

The reason for this result becomes clear when one analyses the sections of the cross-scalogram and of the co-scalogram at the two dominating frequencies (Figure 5). Indeed, the contribution of the energy at 15 Hz to the co-scalogram is practically always negative; conversely, the energy at 29 Hz produces both positive and negative peaks in the co-scalogram, and this gives an appreciable contribution to the filter mask based on the absolute values, but an almost negligible time integral value.

A further confirmation and a quantitative assessment of this behaviour may be obtained by analysing the sections of the *WLCC* maps at the dominating frequencies, which give the time variation of the relevant contribution to the correlation coefficient.

Table 1
Statistics of the *WLCC* maps sections

Point 1	*Global values*		*Filtered values*	
f (Hz)	*Mean*	*RMS*	*Mean*	*RMS*
29	-.580	.487	-.737	.228
81	-.745	.352	-.835	.176
Point 2	***Global values***		***Filtered values***	
f (Hz)	*Mean*	*RMS*	*Mean*	*RMS*
15	-.644	.469	-.833	.215
29	-.033	.687	-.048	.684

Table 1 shows, for the two analysed points, the mean and rms values of *WLCC*, evaluated both considering the complete sections at the dominating frequencies and the portions of the sections remaining after filtering with a mask obtained by thresholding the modulus of the cross-scalogram (threshold level = 150% of the map average), thus excluding the contribution to *WLCC* of low-energy fluctuations. The mean values give the contribution of the considered frequencies to the correlation coefficient, and should be compared with the correlation coefficients of the complete u and v signals, which are –.441 for point 1 and –.332 for point 2. The different behaviour of the dominating frequencies for the two points is clear from the table. Particularly striking is the fact that, while in general the effect of the filter is to increase the mean value and to reduce the rms one, this does not happen for the higher frequency of point 2. Moreover, the contribution of this frequency to *WLCC* is characterized by a negligible mean value and by a very high rms value.

All these results may be given a physical interpretation by referring to the previous findings of Onorato et al. (1997), who observed that high values of the u-v correlation are present in the roll-up and pairing regions, where the vorticity structures are inclined to the flow. On the other hand, the passage of almost round rolled-up vortices, although giving rise to high velocity fluctuations, produces axial and radial velocity signals that are generally nearly orthogonal. Thus, from the present analyses one may infer that in point 2 the 15 Hz frequency is probably connected with pairing vortices. Conversely, the oppositely-signed contributions of the 29 Hz frequency to the u-v correlation are consistent with the passage of vortical structures with an irregularly round shape, and thus having a prevailing inclination which changes almost randomly from the positive to the negative direction with respect to the flow.

CONCLUSIONS

The results of the present analyses confirm that processing procedures based on the wavelet transform may be a useful tool for the analysis of experimental velocity signals acquired in a developing turbulent flow. Indeed, they allow the contribution of different frequencies to various statistical quantities to be followed in time. It is thus possible to ascertain if frequencies contributing to the energy of a velocity fluctuation also contribute to the correlation with another velocity component. Moreover, one may verify if a low Reynolds stress value derives from a continuously small contribution to correlation or from an intermittent one, oscillating between positive and negative values. This may give clues on the dynamics of the vortical structures dominating a certain flow, and on the evolution of the consequent mixing processes.

In this paper the interpretation of the results was guided by the experience gained from a previous DNS of the same coaxial jet at lower values of *Re*. In particular, the different contributions of the various frequencies to energy and Reynolds stresses were found to be consistent with their connection with the dynamics of the vortical structures that had been found from the numerical simulations.

In conclusion, the time-frequency information provided by the wavelet analysis seems to be promising for devising methods to recognize flow features that are not evident from a conventional Fourier analysis. Eventually, this might hopefully lead to the definition of procedures to characterize flows with different degrees of turbulence development, and help in the derivation of more realistic models of turbulence.

Acknowledgements

The present work was financially supported by the Italian Ministry of University and Research, M.U.R.S.T. The authors wish also to thank A. Talamelli, M. Tavanti and G. Tanzini for providing the velocity signals and visualizations obtained in the ENEL-CRT laboratories, and A.M. Di Banella for her invaluable contribution to the processing of the signals and preparation of the figures.

References

Buresti, G., Petagna, P., and Talamelli, A., 1998, "Experimental Investigation on the Turbulent Near-Field of Coaxial Jets," *Experimental Thermal and Fluid Science,* Vol. 17, pp. 18-26.

Daubechies, I., 1992, "Ten Lectures on Wavelets," CBMS-NSF Regional Conference Series in Applied Mathematics, SIAM, Philadelphia.

Farge, M., Kevlahan, N., Perrier, V., and Goirand, E., 1996, "Wavelets and Turbulence," *Proc. of IEEE*, Vol. 84, pp. 639-669.

Li, H., 1998, "Identification of Coherent Structure in a Turbulent Shear Flow with Wavelet Correlation Analysis," ASME *Journal of Fluid Engineering*, Vol. 120, pp.778-785.

Onorato, M., Salvetti, M.V., Buresti, G., and Petagna, P., 1997, "Application of a Wavelet Cross-Correlation Analysis to DNS Velocity Signals," *European Journal of Mechanics B/ Fluids*, Vol. 16, pp. 575-597.

Perrier, V., Philipovitch, T., Basdevant, C., 1995, "Wavelet Spectra Compared to Fourier Spectra, *J. Math. Phys.*, Vol. 36, pp. 1506-1519.